CAMBRIDGE
UNIVERSITY PRESS

Article

Dervillite from Jáchymov, Czech Republic: a non-harmonic approach to the refinement of atomic displacement parameters of silver

Jakub Plášil[1] (ID), Emil Makovicky[2], Václav Petříček[1] and Pavel Škácha[3]

[1]Institute of Physics of the CAS, v.v.i., Na Slovance 1999/2, 18200 Prague 8, Czech Republic; [2]Department of Geosciences and Resource Management, University of Copenhagen, Østervoldgade 10, DK-1350, Copenhagen K, Denmark and [3]Department of Mineralogy and Petrology, National Museum, Cirkusová 1740, Prague 9, 193 00, Czech Republic

Abstract

A rare silver mineral, dervillite (ideally Ag_2AsS_2), has been found in specimens from the famous Jáchymov mining district, Czech Republic. It occurs as very rare long-prismatic crystals up to 0.4 mm across in association with proustite, bismuth and native silver in the thin arsenic veinlets within the Trojická vein (Svornost mine). Dervillite is monoclinic, space group Pc, with $a = 9.6375(3)$, $b = 12.9462(4)$, $c = 6.8497(2)$ Å, $\beta = 99.510(2)°$ and $V = 842.88(2)$ Å^3 ($Z = 8$). The new structure refinement, $R_1 = 2.94\%$ for 18767 reflections with $[I > 3\sigma(I)]$ and $wR_2 = 7.93\%$ for all 20050 reflections, provided a better fit to the data compared to earlier studies, revealing that silver (8 symmetrically independent atomic sites), which adopts various coordinations (from quasi-linear to tetrahedral) in the structure of dervillite vibrates non-harmonically at room temperature. The Gram-Charlier development, describing the atomic displacement parameters of silver atoms, was used to model their non-harmonic behaviour. A discussion on the use of the approach to the data with limited quality is also provided.

Introduction

Dervillite, Ag_2AsS_2, was first described by Weil (1941) as a mineral consisting of Pb, S and Sb, with possible Bi, from the famous Sainte-Marie-aux-Mines mining district in Vosges, Haut-Rhine Province, France with a later reinvestigation by Bari *et al.* (1983). A complete structural study however had to wait for more than 70 years when Bindi *et al.* (2013) published the complete structure refinement for dervillite based on the single-crystal X-ray diffraction data obtained from a crystal found in the famous Lengenbach quarry in Wallis, Switzerland.

We have reinvestigated the dervillite structure on a crystal from Jáchymov, Czech Republic, paying special attention to the silver atoms and the description of their atomic displacement parameters (ADPs) in detail. Here, we report on employing the Gram-Charlier development to silver's atomic displacement parameters in the dervillite structure.

New occurrence of dervillite from the Jáchymov deposit, Czech Republic

Dervillite was found in the material originating from old workings in the Sv. Trojice, or also Trojická (Holy Trinity) vein, in the vicinity of the crosscut with the Geschieber vein at the Daniel level of the Svornost mine, Jáchymov ore district, Krušné Hory Mts, Czech Republic. Jáchymov ore district is a world-famous locality for ~450 mineral species and a historically important district of Ag + As + Co + Ni + Bi and of U vein-type mesothermal mineralisation (Škácha *et al.*, 2019). The ore veins cut a complex of medium-grade metasedimentary rocks of Cambrian to Ordovician age in the envelope of Variscan granite plutons. Most ore minerals were deposited during Variscan mineralisation from mesothermal fluids (Ondrus *et al.*, 2003a, 2003b). The complex geochemistry of primary mineralisation led to an unusually rich supergene zone, with occurrences of numerous minerals formed during post-mining processes (Ondruš *et al.*, 1997; Škácha *et al.*, 2019).

Seven ore stages were distinguished within the Jáchymov ore field: Sn–W sulfoarsenide, ore-free quartz, carbonate–uraninite, arsenide, arsenic-sulfide, sulfide and post-ore stage. Economically, the most important was the carbonate–uraninite stage for uranium ores and the arsenic-sulfide for silver ores. The Trojická vein is one of the typical constituents of the oldest Sn–W sulfoarsenide stage. This stage is related to the auto-metamorphism of younger
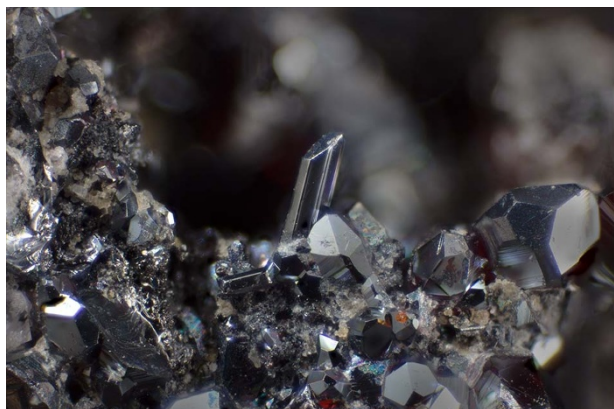
Figure 1. Dervillite prismatic crystal (~0.4 mm across) associated with multi-faceted proustite crystals from Jáchymov. Photo by P. Škácha.

Table 1. Chemical composition (in wt.%) for dervillite ($n = 12$) and proustite ($n = 8$) from Jáchymov as determined by electron microprobe (WDS).

		Mean	Range	S.D.
Dervillite	Ag	58.99	58.52−59.89	0.38
	Cu	0.86	0.80−0.93	0.04
	As	21.00	20.81−21.31	0.18
	Te	0.07	0.00−0.11	0.04
	S	17.48	17.34−17.66	0.11
	Cl	0.03	0.00−0.08	0.03
Proustite	Ag	64.85	64.51−65.21	0.26
	Sb	0.21	0.00−0.74	0.26
	As	14.76	14.39−14.96	0.18
	Te	0.07	0.00−0.13	0.05
	S	18.75	18.63−18.93	0.09
	Cl	0.06	0.00−0.08	0.02

Notes: S.D. – standard deviation; WDS – wavelength dispersive spectroscopy.

granite, which underlies the whole district and has no relation to the younger five-element mineralisation (Ondruš *et al.*, 2003b).

Mineralisation containing the dervillite currently investigated was identified in several ore vein fragments. The mineral itself was found in a vein of native arsenic. The vein is up to 2 cm thick and locally brecciated, enclosing tiny fragments of mica-schists. The oldest mineral in the association is skeletal or fine-grained native silver in aggregates up to 5 mm, sometimes naturally etched from the native arsenic. Arsenic also encloses rare small cubes of violet fluorite. Rare cavities host thick pyramidal dark red proustite crystals up to 2 mm in size, very rarely associated with dervillite. Black prismatic dervillite crystals with strong metal lustre up to 0.5 mm occur only rarely (Fig. 1). It replaces proustite along with usually fine-grained native bismuth, which further replaces both dervillite and proustite. Supergene arsenolite forms up to 2 mm large octahedra or their aggregates and covers the rock fragments containing native arsenic. It also sometimes fills fractures.

Chemical composition

Chemical analyses of dervillite and closely associated proustite were performed using a Cameca SX100 electron microprobe operating in wavelength-dispersive mode (20 kV, 20 nA and 1 µm beam size). The following standards and X-ray lines were used to minimise line overlaps: Ag (Ag$L\alpha$); Bi (Bi$L\alpha$); Bi$_2$Se$_3$ (Se$L\beta$); Cd (Cd$L\alpha$); chalcopyrite (Cu$K\alpha$, Fe$K\alpha$, S$K\alpha$); FeAsS (As$K\beta$); HgS (Hg$L\alpha$); NaCl (Cl$K\alpha$); PbS (Pb$M\alpha$); Sb$_2$S$_3$ (Sb$L\beta$); Sn (Sn$L\beta$); and ZnS (Zn$K\alpha$). Peak counting times were 20 seconds for all elements and 10 seconds for each background. Cadmium, Fe, Pb, Bi, Ni, Co, Au, Se, Sn and Zn were found to be below the detection limits (0.01–0.05 wt.%). Raw intensities were converted to the concentrations of elements using the automatic 'PAP' (Pouchou and Pichoir, 1985) matrix-correction procedure.

With the exception of Cl and Te contents, which are only slightly above the detection limits, Sb and Cu were the only other additional elements to be found in the analysis of the two phases (Table 1), with Cu preferentially entering the dervillite structure and Sb entering the proustite that is tightly accompanied by dervillite on the specimen studied. Analytical data for dervillite (12 analyses) and proustite (8 analyses) are given in Table 1. Based on 5 atoms per formula unit (apfu), the empirical formula for dervillite from Jáchymov is Ag$_{1.97}$Cu$_{0.05}$As$_{1.01}$S$_{1.96}$. On the basis

of 7 apfu, the empirical chemical formula for the studied proustite closely associated with dervillite is Ag$_{3.03}$(As$_{0.99}$Sb$_{0.01}$)$_{3.00}$S$_{2.95}$Cl$_{0.01}$.

Single-crystal X-ray diffraction

A dervillite crystal of the approximate dimensions $0.128 \times 0.038 \times 0.014$ mm was examined at room temperature using a Rigaku SuperNova single-crystal diffractometer. The diffraction experiment was done using Mo$K\alpha$ radiation ($\lambda = 0.71073$ Å) from a micro-focus X-ray tube collimated and monochromatised by mirror-optics and detected by an Atlas S2 CCD detector (2×2 pixels binning). According to single-crystal X-ray data dervillite is monoclinic, with *P*-centred unit cell: $a = 9.6375(3)$, $b = 12.9462(4)$, $c = 6.8497(2)$ Å, $\beta = 99.510(2)°$ and $V = 842.88(2)$ Å^3 (Table 2). Corrections for background, Lorentz, polarisation effects, and absorption correction were applied during data reduction in the *CrysAlis* (Rigaku, 2024) package.

Structure refinement proceeded in the *Jana2020* program (Petříček *et al.*, 2023), employing the model of Bindi *et al.* (2013). Following the previous structure determination, dervillite has been found to crystallise in a non-centrosymmetric monoclinic space group *Pc* (Table 2). The refined Flack parameter, 0.169(7), is very similar to the configuration of the structure studied by Bindi *et al.* (2013). Crystal structure refinement that included all atoms refined with anisotropic displacement parameters returned very acceptable *R* values: $R_1 = 3.41\%$ for 18767 reflections with $I > 3\sigma(I)$ and $wR_2 = 8.70$ for all 20050 reflections with a goodness-of-fit of 1.76 for all reflections. Nonetheless, several difference-Fourier maxima ($\Delta\rho_{max} = 1.87$ e^- Å^{-3}) remained undescribed after the final refinement cycle. They all were found to be close to the silver atoms; the highest of them was located 0.92 Å from Ag6. Inspection of the difference-Fourier maps showed that this remaining electron density, connected with the silver atoms, cannot be described by the simple harmonic approach to the atomic displacement parameters. Therefore, the non-harmonic displacement parameters were implemented for refinement and were modelled as the Gram-Charlier third-order development (see, e.g. Volkov *et al.*, 2023) of the ADPs. At the initial stage, all the Ag atoms were considered and checked carefully for the significance of the variable changes (as $\Delta(param)/\sigma(param)$). Only those atoms with a significant contribution of the non-harmonicity to the atomic displacement were considered in the final model. We employed Wilson's correction to prevent statistical bias in the least-squares

Table 2. Summary of data collection and refinement for dervillite from Jáchymov.

	Harmonic refinement	Non-harmonic refinement
Structural formula (sum)	$Ag_2(As_{0.973}Sb_{0.027})S_2$	$Ag_2(As_{0.976}Sb_{0.024})S_2$
a, b, c [Å], β [°]	9.637(2), 12.946(3), 6.850(2), 99.51(3)	
V [Å³]	842.9(4)	
Space group	—— Pc ——	
Z	8	
$D_{calc.}$ [g.cm⁻³] for the above formula	5.612	5.608
Temperature		
Wavelength	Mo$K\alpha$, 0.71073 Å	
Crystal dimensions	—— 128 × 38 × 14 µm ——	
Limiting θ angles (Completeness to θ_{max})	2.66°–28.07° (97%)	
Limiting Miller indices	$-12 \leq h \leq 12, -16 \leq k \leq 17, -8 \leq l \leq 9$	
No. of reflections measured	20084	20084
No. of unique reflections	20050	20050
No. of observed reflections (criterion)	18767 [$I_{obs}>3\sigma(I)$]	18767 [$I_{obs}>3\sigma(I)$]
Absorption correction (mm⁻¹)	17.806	17.811
F_{000}	3331	1275
Culled reflections ([$I_{culled}>20\sigma(I)$])	34	34
Parameters refined, restraints, constraints	187, 0, 38	267, 0, 38
R, wR^2 (obs)	0.0341, 0.0848	0.0294, 0.0774
R, wR^2 (all)	0.0362, 0.0870	0.0312, 0.0793
GOF obs/all	1.77/1.76	1.62/1.61
$\Delta\rho_{min}, \Delta\rho_{max}$ (e^- Å⁻³); max. charge (e)	−1.35/1.87 (0.92 Å to Ag6), 0.58	−0.40/0.54 (0.87 Å to Ag4), 0.25
Weighting scheme, weights	σ, w = $1/[\sigma^2(F_o^2)+(0.02P)^2]$, $P = (F_o^2+2F_c^2)/3$	σ, w = $1/[\sigma^2(F_o^2)+(0.02P)^2]$, $P = (F_o^2+2F_c^2)/3$
Extinction coefficient (B-C type) *	226(13)	262(12)
Flack parameter	0.166(7)	0.169(7)

*Becker and Coppens (1974)

refinement (Wilson, 1976). The final refinement, including all Ag atoms refined with non-harmonic atomic displacement parameters, converged to the $R_1 = 2.94\%$ for 18767 reflections with $I > 3\sigma(I)$ and $wR_2 = 7.93$ for 20050 reflections with a goodness-of-fit of 1.61 for all reflections and $\Delta\rho_{max} = 0.77$ e^- Å⁻³. The experimental and refinement details for both harmonic and non-harmonic approaches are reported in Table 2. Atomic parameters, including non-harmonic terms (Gram-Charlier development), are embedded in the crystallographic information file (cif), deposited with Supplementary Material (see below). Selected interatomic distances calculated from the refined model are provided in Table 3. Programs *Jana2020* (Petříček *et al.*, 2023) and *Vesta3* (Momma and Izumi, 2011) were used to plot the electron density and the isosurface for Ag atoms' atomic displacement parameters (ADPs).

General description of the crystal structure

Despite its simple chemical formula, in agreement with its low symmetry, the crystal structure of dervillite contains eight independent silver positions, four distinct arsenic sites, and eight different sulfur sites.

The dervillite structure is divided into thick (010) slabs with a complex internal structure. The (010) planar gaps separate the slabs, which are bridged over and interconnected only by Ag–S bonds; these bind together the planar slab surfaces. Perpendicular to this scheme and conspicuous in the [001] projection, the structure is formed by (100)-oriented Ag-predominant portions with wavy character (these are layers with a complex configuration, Figs 2 and 3), which alternate with continuous (100) interlayers distinguised by the predominant role of lone-electron pairs of arsenic (Figs 2, 3, and in detail Fig. 4). In most cases,

the lone-electron-pairs (LEPs) interact with opposing Ag atoms, resulting in lone-electron-pair micelles of unusual type. In their (100) interlayer, adjacent micelles are separated by short intervals containing Ag–S bonds (Figs 3, 4). The shortest Ag–Ag contacts observed in the structure, of ∼3 Å in length, are limited to the Ag-concentrating layers (Fig. 5a), whereas the short, strong As–As bonds are situated in the surfaces of the LEP-based interlayers (detailed view in Fig. 4a,b).

The sub-sulfide character of dervillite (Bindi *et al.*, 2013) is thus demonstrated by a combination of As–As bonding, involvement of Ag in interactions with LEPs of As, and by at least one example of weak cation–cation (i.e. Ag–Ag) interaction. In the As–As pair, the covalent bond consumes two electrons, and the As–As group functions as two divalent cations. With 4 Ag pfu added, the charge of four S^{2-} becomes compensated.

Ag-based polyhedra

The bulk of silver atoms comprises nearly tetrahedral coordination, mostly with additional complications or variations.

Ag1 and Ag5 are tetrahedra, with all four corners occupied by sulfur (Table 3). Bond lengths vary between 2.556 Å and 2.665 Å, exceptionally reaching 2.700 Å. There is an additional Ag–Ag contact at 3.096 Å between Ag1 to Ag6. The Ag3 is a tetrahedron with three sulfurs and one As/Sb as vertices (Figs 3 and 6b).

Ag2 is in a [3]-coordinated near-to-planar arrangement by three S atoms (S3 and 2× S7) and additionally by one bond to As1/Sb1 (via LEP) and a Ag–Ag contact Ag5 (3.216 Å), forming a distorted tetragonal bipyramid (including Ag) or trigonal pyramid (including just As/Sb coordination). Ag4 is a tetrahedron with all ligands represented by S atoms.

Table 3. Selected interatomic distances (in Å) in dervillite from Jáchymov.

Ag atoms						As/Sb atoms	
Ag1–S2	2.596(2)	Ag4–S1^{iv}	2.6712(19)	Ag7–S3^{v}	2.855(2)	As1/Sb1–As4	2.4939(12)
Ag1–S2^{i}	2.6451(17)	Ag4–S3^{iv}	2.5916(17)	Ag7–S4^{v}	2.520(2)	As1/Sb2–S2^{iii}	2.2411(17)
Ag1–S5	2.6366(17)	Ag4–S4	2.556(2)	Ag7–S5	2.409(2)	As1/Sb3–S5	2.2357(17)
Ag1–S7	2.5802(19)	Ag4–S4^{ix}	2.6208(17)	Ag7–Ag8	3.017(2)		
Ag1–Ag6	3.0979(18)						
		Ag5–S2	2.645(2)	Ag8–S8	2.430(2)	As2/Sb2–As3	2.5054(12)
Ag2–S3^{ii}	2.5180(19)	Ag5–S3^{xiv}	2.6987(18)	Ag8–S8^{ix}	2.391(2)	As2/Sb2–S3	2.2473(18)
Ag2–S7	2.5073(19)	Ag5–S6^{xiv}	2.558(2)	Ag8–Ag8^{viii}	3.431(3)	As2/Sb2–S4	2.2543(17)
Ag2–S7^{ii}	2.646(2)	Ag5–S6^{xv}	2.6642(18)				
Ag2–As1/Sb1^{ii}	2.8003(15)	Ag5–Ag7^{iv}	3.1873(18)			As3/Sb3–S6	2.2480(18)
						As3/Sb3–S7	2.2139(17)
Ag3–S1	2.595(2)	Ag6–S2	2.833(2)				
Ag3–S1^{ix}	2.4802(17)	Ag6–S6^{v}	2.435(2)			As4/Sb4–S1	2.2194(17)
Ag3–S5	2.4925(17)	Ag6–S8^{iv}	2.504(2)			As4/Sb4–S8	2.2777(17)
Ag3–As2/Sb2	2.7116(12)						

Symmetry codes: (i) *x*, −*y*+2, *z*−½; (ii) *x*, −*y*+2, *z*+½; (iii) *x*, *y*, *z*−1; (iv) *x*, *y*, *z*+1; (v) *x*+1, *y*, *z*; (vi) *x*−1, *y*, *z*−1; (vii) *x*−1, −*y*+2, *z*−½; (viii) *x*, −*y*+1, *z*−½; (ix) *x*, −*y*+1, *z*+½; (x) *x*−1, *y*, *z*; (xi) *x*−1, *y*, *z*+1; (xii) *x*−1, −*y*+1, *z*+½; (xiii) *x*, −*y*+1, *z*+3/2; (xiv) *x*+1, *y*, *z*+1; (xv) *x*+1, −*y*+2, *z*+½.
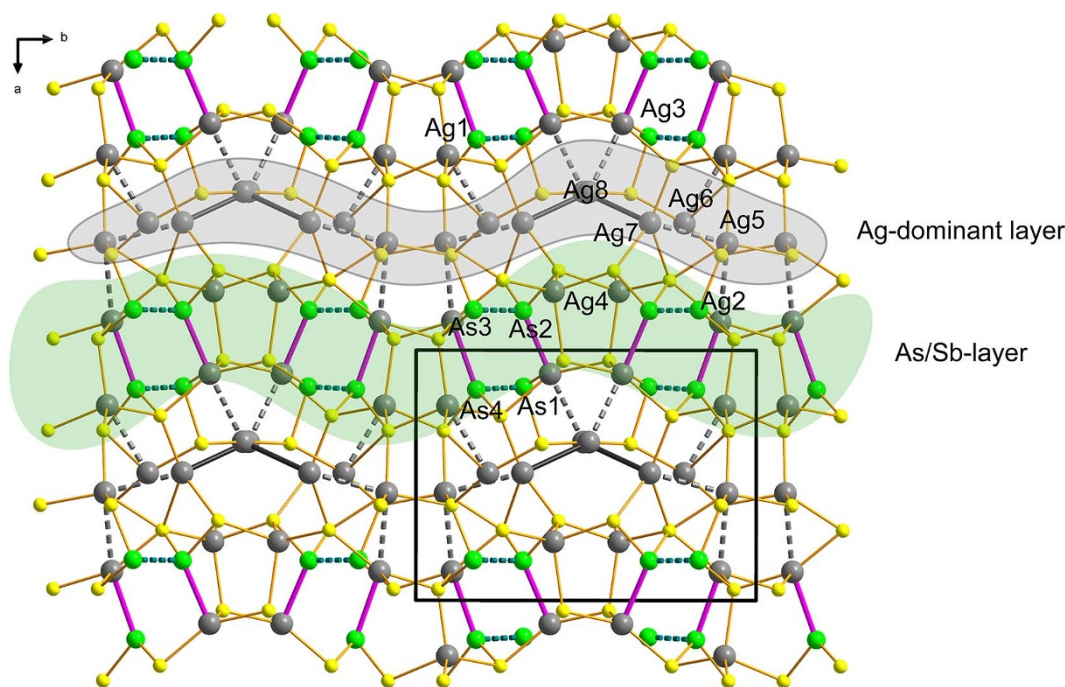

Figure 2. Crystal structure of dervillite viewed down **c** approximately (slightly inclined) using ball-and-stick presentation. S: yellow; Ag: dark grey, As: green. Cation pairs As–As (dashed teal-coloured line representing covalent bonds), Ag–As (purple-coloured interaction of lone-electron pair of As with Ag), and Ag–Ag (grey-coloured joins representing metal–metal interactions; dashed grey lines indicate close metal–metal contacts: Ag1–Ag6 = extra sheet contact, Ag3–Ag8 = extra sheet contact, Ag5–Ag7, Ag7–Ag8) in dervillite. Unit-cell edges outlined in black solid lines. All structures drawn using *Vesta* (Momma and Izumi, 2011).

Ag6 is in trigonal planar configuration (S2, S6, S8; 2.43–2.83 Å) with an additional Ag–Ag contact to Ag1 (3.097 Å). Ag7 is also in trigonal coordination by three S atoms (S3, S4, S5; 2.41–2.86 Å) plus two Ag–Ag contacts: to Ag5 (3.188 Å) and Ag8 (3.016 Å). Ag8 is a pseudo-linear configuration, plus a side-bond to Ag7 (3.016 Å) that completes a triangle. A close contact to Ag3 (3.174 Å) should be also mentioned here, on the opposite side from Ag7. The linear-disposed S–Ag–S bonds are 2.394 Å and 2.428 Å.

Arsenic

All arsenic atoms in the structure are paired by a covalent bond, with an As–As distance between 2.493 Å and 2.506 Å (Figs 5a,b).

In the weaker As–As interactions range, As2 and As3 more or less face one another with their LEPs (Fig. 4b). Bindi *et al.* (2013) noted that As1 and As4 face and react with the opposing Ag atoms. Apparently, the LEPs of arsenic and orbitals of Ag react (always as an As–Ag pair, one by one) and reduce the As–Ag distance to only 2.716 Å or slightly above this value. The Ag–As interaction via LEPs of arsenic (donation to the Ag orbitals, see Bindi *et al.*, 2013) is comparable to the 2.65 Å long Cu–LEP(As) interaction in spaltiite $Cu_2Tl_2As_2S_5$ (Graeser *et al.*, 2014, illustrated in Makovicky, 2018) which also contains modified LEP micelles which are reminiscent of those in the present structure. The short covalent As–As bonding present in dervillite deserves comparison with other similarly behaving subsulfides such as the mineral lautite, CuAsS (Bindi
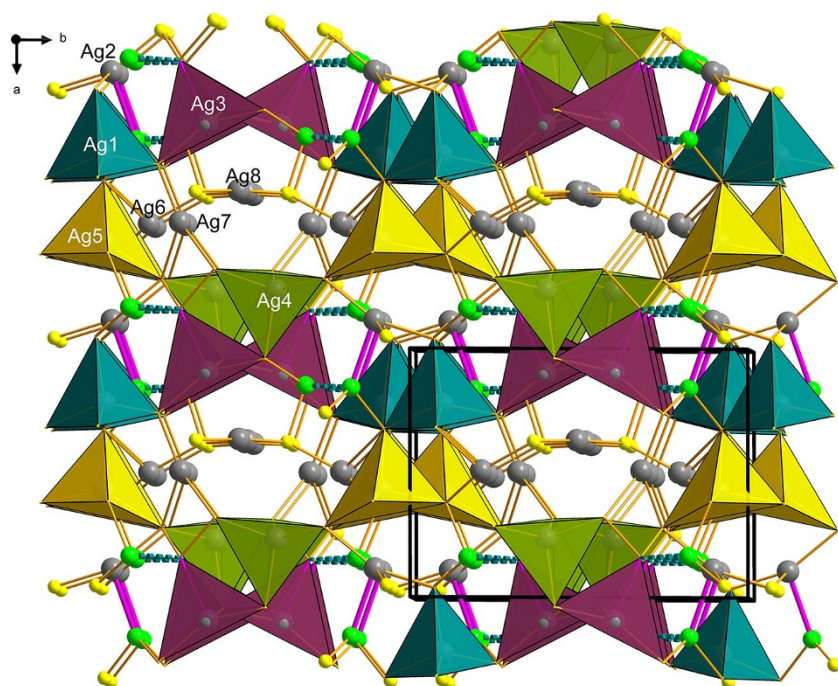
Figure 3. Projection of the crystal structure of dervillite along *c*, showing coordination of silver atoms. Tetrahedrally coordinated: Ag1, Ag3, Ag4, Ag5; triangular coordination Ag2, Ag6, Ag7, Ag8. Dashed lines represent As–As (LEPs), violet solid lines Ag–As interactions.
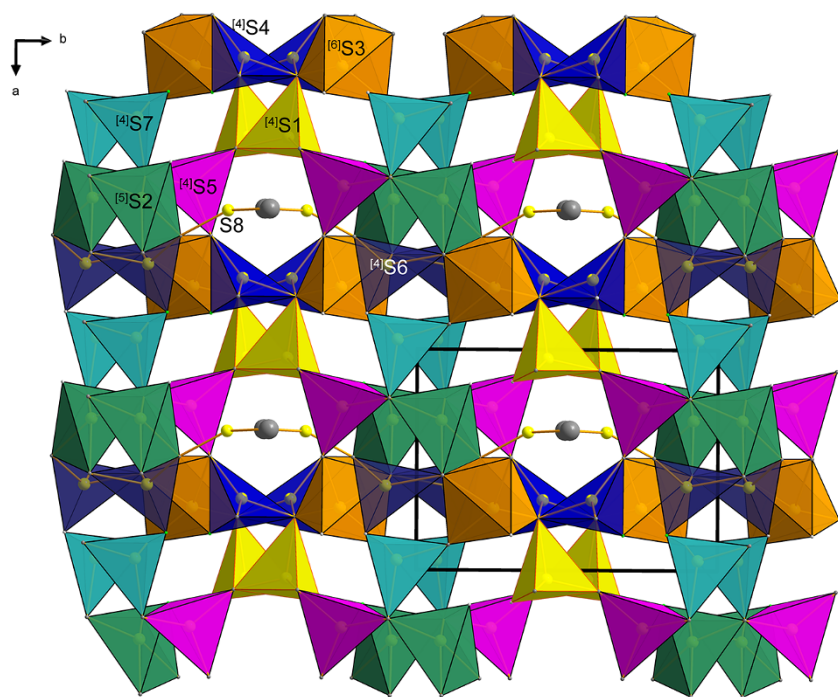

Figure 4. S-based polyhedra in the crystal structure of dervillite. Polyhedra for the S8 atom is omitted for clarity, but it is [4]-coordinated (As4, 2×Ag8, Ag6). Cation–cation interactions are also omitted for clarity.

et al., 2008) (As–As = 2.4965(8) Å), the As–S molecular compounds (e.g. dimorphite: 2.46–2.48; realgar: 2.56–2.57; pararealgar: 2.48–2.53 Å, uzonite: 2.50–2.58 Å; see Bonazzi and Bindi, 2008; wakabayashilite: 2.656 Å, Bonazzi *et al.*, 2005), with complex sulfosalt sterryite (2.63 Å; Moëlo *et al.*, 2012), or even with the covalently bonded As in the structure of arsenic (Wyckoff, 1963; As–As = 2.506 Å). As Bindi *et al.* (2013) pointed out, the weak Ag–As bonds in dervillite, of a dative covalent bond (As lone pair to the closed-shell d^{10} Ag cations), secure the kind of '*anionic*' character of the dervillite structure.

S-based tetrahedra

Regarding sulfur-centred coordination polyhedra, S-based tetrahedra are the principal polyhedral element of the crystal structure of dervillite (Fig. 6). Among the sulfur atoms, S1, S4, S5, S6, S7 and S8 are in tetrahedral coordination by 3 Ag + 1 As. These tetrahedra are all flattened by the central S atom being shifted towards the triangular Ag$_3$ base, which opposes the short S–As bond (the only one of the short As–S bonds per S atom). Unlike these six sulfurcentred polyhedra, the S2 site is in a square pyramid with As as the apical vertex (4 Ag + 1 As), and S3 in an octahedron formed
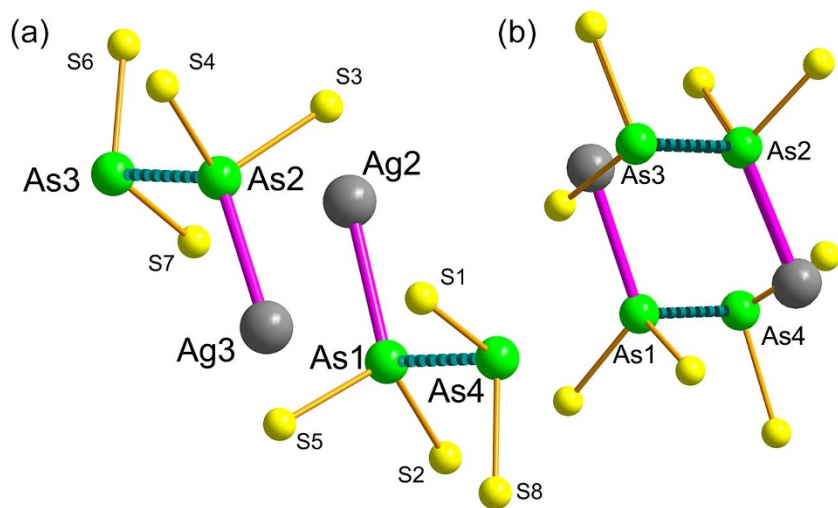
Figure 5. The LEP-bonded arsenic–silver slab from the crystal structure of dervillite with Ag intercalations. (a) A side-view on As–As pairs and their bonding environments. (b) The view is perpendicular to the previous one with overlapping As–As joins and LEP micelles
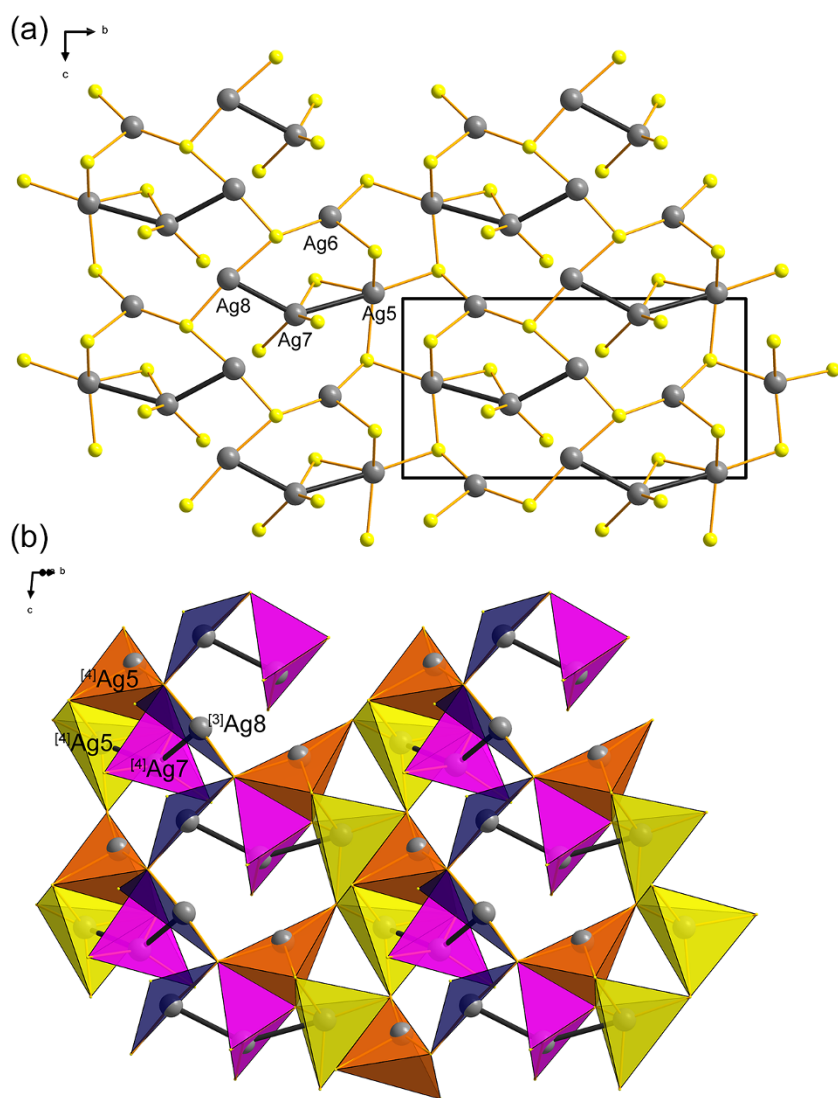

Figure 6. The complex silver-rich wavy (100) layer from the crystal structure of dervillite: (a) Ball-and-stick model; and (b) polyhedral model. Ag1, Ag2, Ag3 and Ag4 are not present within this layer. The dark-grey bond represents Ag–Ag interactions.
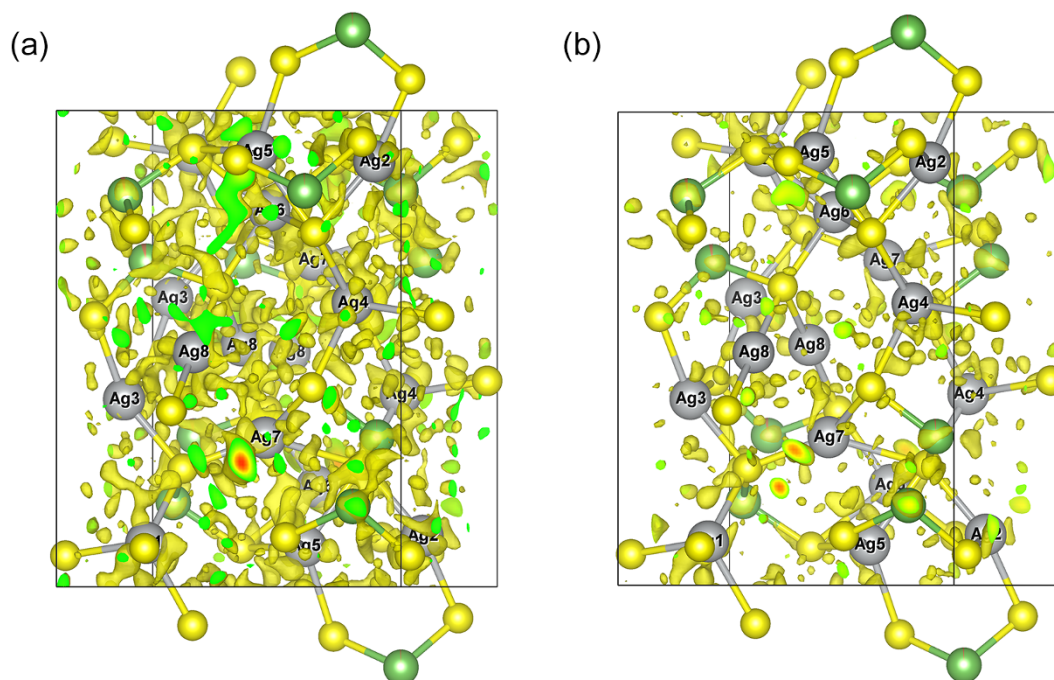
Figure 7. Difference-Fourier 3D maps plotted for the entire unit cell of dervillite. (a) Harmonic vs. (b) non-harmonic refinement. The isosurface level is set to the same value (0.25).
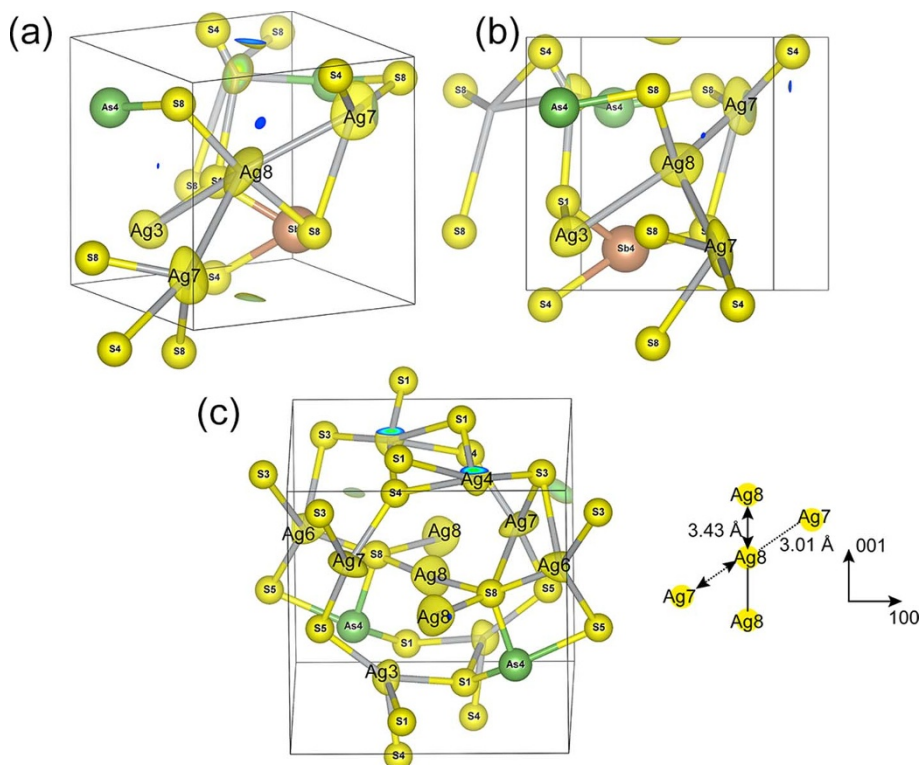

Figure 8. Three different projections providing a view of the non-harmonic atomic displacement parameters of Ag in the structure of dervillite (represented by the j.p.d.f. isosurface). The metal–metal interactions are displayed as dark-grey joins, and the size of the S, As/Sb atoms is set arbitrarily. Noteworthy is a pseudo-linear arrangement of the Ag8–Ag8 atoms in the structure (extending along c) and 'diagonally' arranged interacting Ag7 atoms (approximately in a plane). The highest mobility of the silver (diffusion) could be expected there at non-ambient temperatures. The j.p.d.f. calculations by *Jana2020* and plotted by *Vesta3*. The isosurface level of the 3D maps is 0.05 Å^{-3}.

by 5 Ag + 1 As. As2 and As3 more or less face one another with their LEPs, whereas As1 and As4 face, and *via* their LEPs react, with the opposing Ag atoms (always as a pair As–Ag). The regular presence of one As–S bond in every coordination polyhedron of S is typical for dervillite and demonstrates evenness of local charge compensation throughout the structure.

Structural adjustments to the sub-sulfide character

An exciting aspect of the dervillite structure is a conversion of the As–S–As distance to As–As distance by weakening the As–S interconnections. The average As–As bond in dervillite is 2.5 Å long whereas the average As–S distance is ~2.24 Å. Thus, the 'full-sulfide' As–S–As distance of 4.48 Å will be reduced to 2.5 Å, i.e. with a loss of 1.98 Å. The directions in question are diagonal to the *b* parameter so that the length loss on the *b* dimension can be estimated at ~1.5 Å or more (Figs 2, 3, 5a,c).

Looking at the position of As–As vectors in the structure (e.g. Fig. 2), they are situated in the (100) planes and centred on *y* = 0.25 and 0.75. Furthermore, especially the As–Ag interactions define a general herringbone orientation of bonds, which is also expressed in a wavy character of (100) layers (Fig. 2). LEP micelles are orientated diagonally in the (010) layers, right and left of the composition planes, which separate adjacent (010) layers.

As an example of a configurational situation, the (100) face of the LEP micelle is formed by Ag3 in tetrahedral coordination and Ag5 in triangular coordination. They are joined by S4, which tops the mentioned face. In the Ag-rich wavy (100) layer, they are followed by Ag6 and Ag8, which are differently coordinated. What is essential is that the two such configurations with converging arrangement/orientation force Ag7 into a linear [001] arrangement, the only linear chain of silver. Ag6 and especially Ag8 are coordinated by S3 positioned on the (100) face of the next LEP micelle along the [100] direction, and then the configuration repeats itself.

The just mentioned (010) composition plane, which amalgamates the herringbone-arranged blocks (at *y* = 0.5, with centrally positioned Ag7, and limited by Ag1–Ag1 positions), differs from that at *y* = 0.0, which lacks a centrally situated Ag atom and is limited by Ag2–Ag2 and Ag3–Ag3 [100] sequences (Fig. 2). Thus, the alternating composition planes differ from one another. The *c*-glide planes are situated in these planes of slab contacts.

Discussion – non-harmonic *vs.* harmonic refinement

Recently, a thorough discussion on the use of harmonic *vs.* non-harmonic atomic displacement parameters has been provided by Plášil *et al.* (2024). The authors also commented in detail on the careful evaluation and handling of the experimental data. It is essential to adequately consider how much 'non-harmonicity' could be used in the refinement, i.e. up to which order of the Gram-Charlier development we can opt for and use. In the current case, we have decided to keep only the third-order for all the Ag atoms, keeping in mind that the data quality (resolution) is still somewhat limited (for instance, compared to the case of the recently investigated mineral theuerdankite, described by Plášil *et al.*, 2024). The use of a non-harmonic approach of the ADPs of all Ag atoms in dervillite provided much cleaner (and also meaningful) difference-Fourier maps (compare Figs 7a and 7b), although the drop in the *R*-values is not the 'rocket' one. A large number of the Ag atoms behave/vibrate in the same fashion in the structure of dervillite, but to a greater or lesser extent. Generally, the atoms vibrate perpendicular to the actual bonds (Ag–S) (Fig. 8). The effect of the non-harmonicity is namely apparent for Ag7 and Ag8 atoms (Fig. 8a–c). Noteworthy, from the j.p.d.f. (joint-probability-density function) maps, it seems that the Ag3–Ag8 interaction might be more favoured than for Ag7–Ag8, despite the distances for the first mentioned pair being somewhat longer (3.17 for Ag for the Ag3–Ag8 *vs.* 3.01 Å for Ag7–Ag8). None of

the silver atoms at room temperature is highly mobile in dervillite; nevertheless, all silver atoms in the dervillite structure are 'non-harmonically vibrating'. The non-harmonic refinement of all Ag atoms in the structure of dervillite led to a reasonable and better model-to-data fit. The improvement is not apparent at first glance from the quick drop of *R*-values, but it is obvious from the difference-Fourier maps. We can expect greater Ag mobility at higher temperatures, namely for the Ag7–Ag8 join (maybe Ag3?) (check particularly Fig. 8c). However this should be a subject for the subsequent temperature-dependent diffraction study.

Competing interests. The authors declare none.

References

Bari H., Cesbron F., Moëlo Y., Permingeat F., Picot P., Pierrot R., Schubnel H.J. and Weil R. (1983) La dervillite, Ag$_2$AsS$_2$, nouvelle définition de l'espèce. *Bulletin de Minéralogie*, **106**, 519–524.

Becker P.J. and Coppens P. (1974) Extinction within the limit of validity of the Darwin transfer equations. I. General formalism for primary and secondary extinction and their applications to spherical crystals. *Acta Crystallographica*, **A30**, 129–147.

Bindi L., Catelani T., Chelazzi L. and Bonazzi P. (2008) Reinvestigation of the crystal structure of lautite, CuAsS. *Acta Crystallographica*, **E64**, i22.

Bindi L., Nestola F., De Battisti L. and Guastoni A. (2013) Dervillite, Ag$_2$AsS$_2$, from Lengenbach quarry, Binn valley, Switzerland: occurrence and crystal structure. *Mineralogical Magazine*, **77**, 3105–3112.

Bonazzi P. and Bindi L. (2008) A crystallographic review of arsenic sulfides: Effects of chemical variations and changes induced by light exposure. *Zeitschrift für Kristallographie*, **223**, 132–147.

Bonazzi P., Lampronti G.I., Bindi L. and Zandari S. (2005) Wakabayashilite, [(As,Sb)$_6$S$_9$][As$_4$S$_5$]: crystal structure, psuedosymmetry, twinning, and revised chemical formula. *American Mineralogist*, **90**, 1108–1114.

Graeser S., Topa D., Effenberger H., Makovicky E. and Paar W.H. (2014) Spaltiite, IMA 2014-012. CNMNC Newsletter No. 20, June 2014, page 557. *Mineralogical Magazine*, **78**, 549–558.

Makovicky E. (2018) Modular crystal chemistry of thallium sulfosalts. *Minerals*, **8**, 478.

Moëlo Y., Guillot-Deudon C., Evain M., Orlandi P. and Biagioni C. (2012) Comparative modular analysis of two complex sulfosalt structures: sterryite, Cu(Ag,Cu)$_3$Pb$_{19}$(Sb,As)$_{22}$(As-As)S$_{56}$, and parasterryite, Ag$_4$Pb$_{20}$(Sb,As)$_{24}$S$_{58}$. *Acta Crystallographica*, **B68**, 480–492.

Momma K. and Izumi F. (2011) VESTA 3 for three-dimensional visualization of crystal, volumetric and morphology data. *Journal of Applied Crystallography*, **44**, 1272–1276.

Ondruš P., Veselovský F., Skála R., Císařová I., Hloušek J., Frýda J., Vavřín I., Čejka J. and Gabašová A. (1997) New naturally occurring phases of secondary origin from Jáchymov (Joachimsthal). *Journal of the Czech Geological Society*, **42**, 77–108.

Ondruš P., Veselovský F., Gabašová A., Hloušek J., Šrein V., Vavřín I., Skála R., Sejkora J. and Drábek M. (2003a) Primary minerals of the Jáchymov ore district. *Journal of the Czech Geological Society*, **48**, 19–147.

Ondruš P., Veselovský F., Gabašová A., Hloušek J. and Šrein V. (2003b) Geology and hydrothermal vein system of the Jáchymov (Joachimsthal) ore district. *Journal of the Czech Geological Society*, **48**, 3–18.

Petříček V., Palatinus L., Plášil J. and Dušek M. (2023) Jana2020 – a new version of the crystallographic computing system Jana. *Zeitschrift für Kristallographie*, **238**, 271–282.

Plášil J., Sejkora J., Dolníček Z., Petříček V., Désor J., Majzlan J., Gross M., Möhn G. and Schürmann Ch. (2024) Theuerdankite, Ag_3AsO_4, a new mineral from the Alter Theuerdank Mine (St. Andreasberg), Germany. *Mineralogical Magazine*, **88**, 557–564.

Pouchou J.L. and Pichoir F. (1985) "PAP" ($\pi\rho Z$) procedure for improved quantitative microanalysis. Pp. 104–106 in: *Microbeam Analysis* (J.T. Armstrong, editor). San Francisco Press, California.

Rigaku (2024) *CrysAlis CCD and CrysAlis RED*. Rigaku–Oxford Diffraction Ltd, Yarnton, Oxfordshire, UK.

Škácha P., Plášil J. and Horák V. (2019) *Jáchymov: mineralogická perla Krušnohoří*. Academia, Praha 682. [in Czech with the English summary].

Volkov S.N., Charkin D.O., Firsova V.A., Aksenov S.M. and Bubnova R.S. (2023) Gram–Charlier approach for non-harmonic atomic displacements in inorganic solids: A review. *Crystallography Reviews*, **29**, 151–194.

Wilson A.J.C. (1976) Statistical bias in Least-Squares Refinement. *Acta Crystallographica*, **A32**, 994–996.

Weil R. (1941) La dervillite, espèce minérale nouvelle. *Revue des Sciences Naturelles d'Auvergne*, **7**, 110–111.

Wyckoff R.W. (1963) *Crystal Structures 1, Second Edition*. Interscience Publisher, Geneva, Switzerland, pp. 7–83.